Silylium ion Migration Dominated Hydroamidation of Siloxy-alkynes

HengdingWang[1,2], Ling Jiang[1,2], HongjunFan[1,2]*.

[1]State Key Laboratory of Molecular Reaction Dynamics, Dalian National Laboratory for Clean Energy, Dalian Institute of Chemical Physics, Chinese Academy of Sciences, Dalian 116023, China

[2]University of Chinese Academy of Sciences, Beijing 100864, China.

ABSTRACT: Intermolecular hydroamidation of internal alkynes has been a long-standing challenge, one of the most successful examples so far is silver-catalyzed hydroamidation of siloxy-alkynes for which meet the standards of atom economic and mild reaction conditions of ideal hydroamidation. However, the mechanism of this reaction remains controversy. Using density function theory (DFT), we revealed that the reaction takes place through a silylium ion migration mediated hydroamidation (SMH) pathway. The SMH pathway goes through two steps, the first step is Ag+ promoted proton and silylium ion exchange between siloxy-alkynes and amide, leading to ketene and silyl-imines, the second step is Ag+ catalyzed nucleophilic addition between ketene and silyl-imines, following with a silylium ion migration afford the final product. In this reaction, Ag+ activate the siloxy-alkyne into silylium ion and silver-ketene through *p*-*π* conjugate effect, the silylium ion then act as catalyst. According to our calculation, the scopes of alkynes in this reaction may be extend to silyl-substituted ynamines or silyl-substituted ynamides, and the scopes of amide maybe expanded into *p*-*π* conjugate system such as diazoles, diazepines and so on. Our calculations also reveal a concise way to construct substituted enamides through Ag+ catalyzed nucleophilic addition between ketenes (or ketene imines) and silyl-substituted *p*-*π* conjugate system such as silyl-imines, silyl-diazoles.

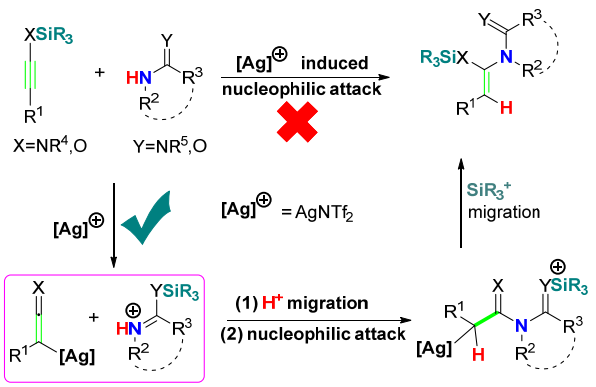

1. Introduction

Hydroamidations have attracted very attentions for it's an atomic-economy way to construct enamides[1-9]. Further, the substrates of this reaction are easily-accessible. Hydroamidations are not spontaneous mainly due to the relatively high barrier of nucleophilic process[10]. Lewis-acid or transition metals are often used to catalyze this reaction. Significant progresses have been made in catalyzed hydroamidation and high levels of chemo-, regio-, and stereo- selectivity have been reported[4, 11-12]. However, current reported successful examples are mainly center on intramolecular hydroamidation[13-16] or hydroamidation involving terminal alkynes[9, 17], and relatively high temperature is required in the most case.

To date, the catalytic variant remains rather limited, especially in hydroamidation of internal alkynes[18-20]. To the best of our knowledge, there were only two hydroamidation reactions of internal alkyne which meet the requirements of atomic economic of ideal hydroamidation[18-19]. Indisputably, make clear the mechanisms of these reactions are very important, for which can provide direct insights to broaden substrate scope and improve efficiency of such reaction.

In 2016, Cui et al. reported first example of hydroamidation of phenyl-substituted alkyne with Ru(II) as catalyst[19]. The reaction proceed under relatively high temperature (90 ℃) and the substrates scope of amides is very limited, only the *N1*-benzyl-*N2,N2*-diisopropyloxalamide and its analogs are suitable for this reaction.

In 2006 Kozmin et al. reported the first example of hydroamidation of internal alkynes[18]. They found that $AgNTf_2$ can promotes the addition of second-amides or carbamates to the triple-bond of siloxy-alkyne successfully in the room temperature within 30 min (Scheme 1a). In this reaction, the *E*-configured Markovnikov product is exclusively obtained. The authors also found that the commonly used ynamides and simple internal alkynes are inactive in the same condition. Based on deuterium label experiment, the author proposed a silver induced nucleophilic addition mechanism (NUA mechanism, Scheme 1b). In this mechanism, the silver(I) coordinated with siloxy-alkyne **1** to form π-complex **INTA**, the amide **2** then nucleophilic attack the siloxy-alkyne **1** to form ***Z*-INTB**. Proton transfer of ***Z*-INTB** lead to final product ***Z*-3**. The nucleophilic attack step is thought to be rate determine step (RDS).

The mechanism complies with some experimental observation, but does not explain why electron-richer ynamides are nonreactive in the same condition, it should be more reactive if this reaction proceed through silver(I) induced nucleophilic attack process[21-23]. Further, the transition metal induced nucleophilic reaction favors take place at trans-direction of metal atom due to the *β*-effect[24].

Scheme 1. Silver(I) catalyzed hydroamidation reported by Kozmin et al.

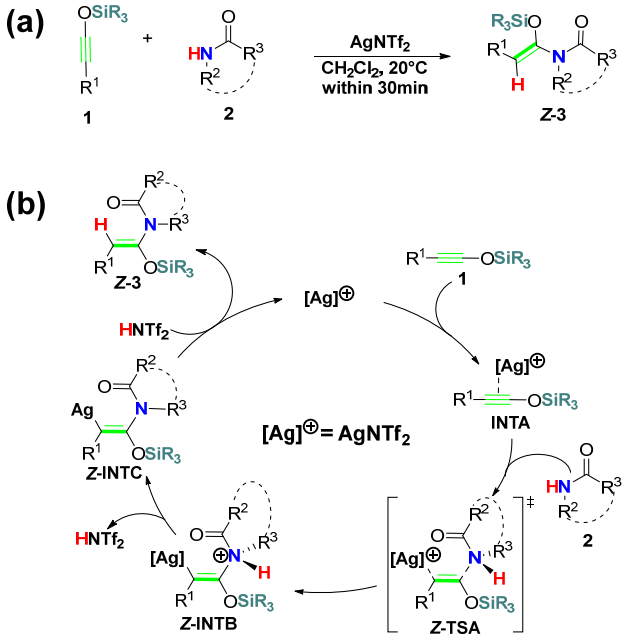

The aims of this study are to find a more reasonable mechanism of this pioneer work to understand, the reactivity, as well as the origins of chemo and regio-selectivity of this reaction. The potential substrates scopes of this reaction have been discussed based on our proposed mechanism.

2. Model reaction

Methyl substituted siloxy-alkyne **1a** and carbamate **2a** was choose as model reaction, $AgNTf_2$ was choose as catalyst. dichloromethane (DCM, ε =8.93) was choose as solvent.

3. Computational details

Density function calculations (DFT) were performed with the Gaussian 16 program package[25]. The structures of **TS1** and **INT1** were optimized in solvent under ωb97xd-SMD/def2-SVP[26-27] level of theory for electron static effect and steric hindrance of triisopropylsilyl (**TIPS**) group make it very hard to load these five coordinated structures in the gas phase[22]. The single point energy of **TS1** and **INT1** was corrected at ωb97xd(gas) /def2tzvpp level of theory, so:

$$G^{sol}_{def2tzvpp} = G^{sol}_{def2svp} - E^{gas}_{def2svp} + E^{gas}_{def2tzvpp} \quad (1)$$

The barrier of formation **TS1** And **INT1** is evaluated with:

$$\Delta G^{sol}_{def2tzvpp} = G^{sol}_{def2tzvpp}(1) - G^{sol}_{def2tzvpp}(0) \quad (2)$$

$G^{sol}_{def2tzvpp}(1)$ refers corrected Gibbs free energy of **TS1** or **INT1**, $G^{sol}_{def2tzvpp}(0)$ refers to corrected Gibbs free energy of reference point **1a**, **2a** and $AgNTf_2$.

The other structural optimizations were performed under ωb97xd(gas)/def2-SVP level of theory. Single point energy was calculated at ωb97xd /def2tzvpp level of theory. Solvation calculations were carried out with SMD solvation model at ωb97xd/def2-SVP level of theory with dichloromethane (DCM, ε =8.93) as solvent. So, in this case, corrected Gibbs energy is:

$$G^{corr\text{-}sol}_{def2tzvpp} = G^{gas}_{def2svp} - E^{gas}_{def2svp} + E^{gas}_{def2tzvpp} + E^{sol}_{def2svp} - E^{gas}_{def2svp} \quad (3)$$

The barrier is evaluated with:

$$\Delta G^{corr\text{-}sol}_{def2tzvpp}(SMD) = G^{corr\text{-}sol}_{def2tzvpp}(1) - G^{corr\text{-}sol}_{def2tzvpp}(0) \quad (4)$$

Our previous work has shown that this scheme is well suitable for evaluate reaction barrier of such system[22]. Actually, $\Delta G^{corr\text{-}sol}_{def2tzvpp}(SMD)$ is a good approximation of $\Delta G^{sol}_{def2tzvpp}$. Vibrational frequency calculations were carried out at same level of theory as geometries optimization to verify that the optimized geometries are energy minimum or transition state and to provide thermal corrections for Gibbs free energies and enthalpies at 298.15 K in 1 atm. IRC calculation was performed for the key transition states to verify that the optimized transition states lead to correct structures[28]. Optimized geometries were rendered with CYLView[29]. The NCI analysis[30] was carried out with Multiwfn[31] and rendered with VMD[32]. The electrophilicity ω index and nucleophilicity N index is calculated with[33] ωb97xd/def2svp level of theory.

$$\omega = \frac{(E_{HOMO} + E_{LUMO})^2}{8(E_{HOMO} - E_{LUMO})} \quad (5)$$

$$N = [E_{HOMO}(Nucleophile) - E_{LUMO}(Tetracyanoethelene)] \quad (6)$$

4. Results and Discussion

4.1. Nucleophilic attack at carbon atom (NUA mechanism).

We evaluate the author proposed NUA mechanism (Figure 1). At beginning of the reaction, coordination of siloxy-alkynes **1a** with the $AgNTf_2$ is exergonic by 10.1kcal/mol (Figure 1a). $AgNTf_2$ coordinate with triple bond of **1a**, makes **1a** susceptible to nucleophilic attack. There are three possible sites to attack **1a**, which is α-C, β-C (Figure 1a) and silicon atom. As for the nucleophilic attack of the two *sp*-hybridized carbon atoms, nucleophilic at α-C position is much more facile due to p-π conjugate effect[22]. So, we only consider nucleophilic attack of the α-C position. There are two directions of nucleophilic attack at α-C

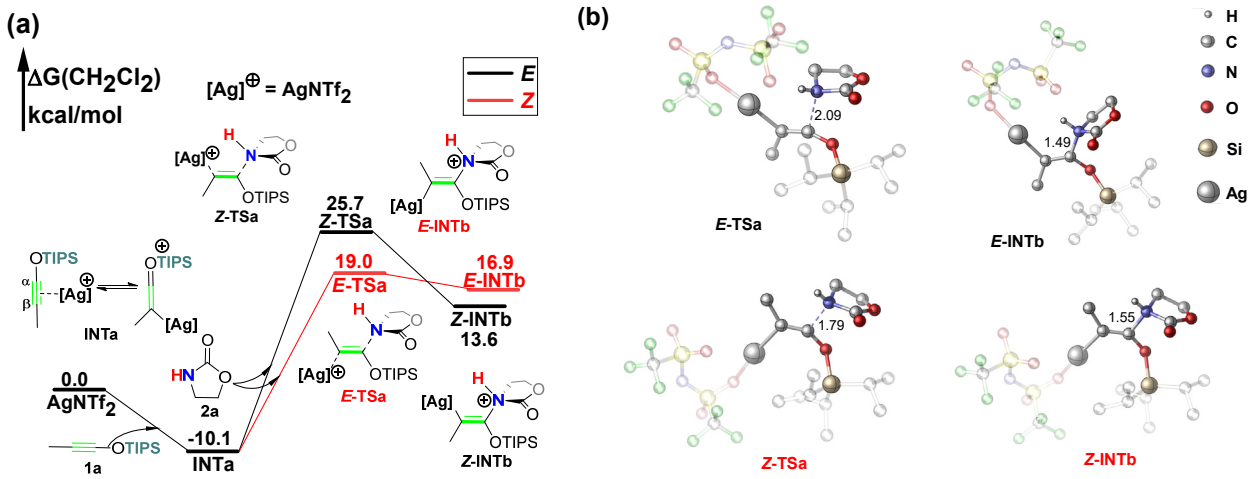

Figure 1. Ag+ induced nucleophilic attack mechanism (NUA mechanism), Gibbs energies are in kcal/mol. **a**. Gibbs free energy profile. **b.** Optimized geometries. The hydrogen atom was omitted, the isopropyl of triisopropylsilyl (TIPS) group and NTf_2^- anion was set to transparent for clarity.

position, if nucleophilic attack take place at the $AgNTf_2$ side, *cis*-addition product ***Z*-3a** will be obtained; otherwise, *trans*-addition product ***E*-3a** will be formed. Our calculation shows that the nucleophilic attack of **2a** prefers take place at opposite side of $AgNTf_2$ which lead to *trans*-conformation product ***E*-3a**, the main cause of the *trans*-selectivity is the *trans*-β effect[24]. The C-N formation leading to ***Z*-3a** is energetically highly disfavored with a barrier (***Z*-TSa**) 35.8kcal/mol, implies that the commonly accepted NUA pathway is disfavored.

4.2. Silylium ion migration dominated hydroamidation (SMH) mechanism.

The nucleophilic attack at silicon atom of siloxy-alkyne is often overlooked for the large size of TIPS group. However this process is quite easy in somecases[22]. Enlighted by our previous work[22], we proposed a silylium ion migration dominated hydroamidation (SMH) mechanism for this reaction (Scheme 2).

Scheme 2. Our proposed silylium ion migration dominated hydroamidation mechanism.

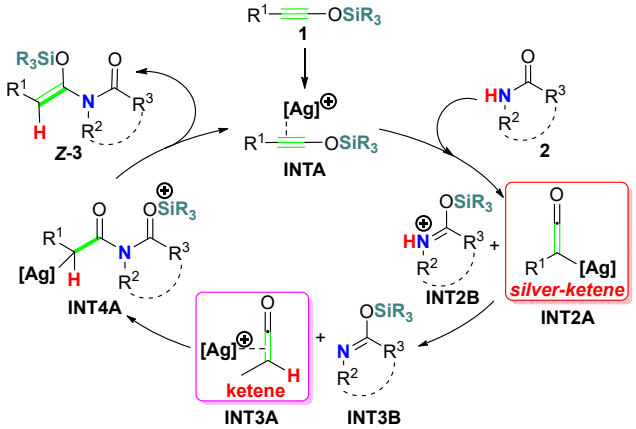

The key feature of the SMH mechanism is Ag+ strong interact with C≡C bond of siloxy-alkynes and activate R_3Si group into silylium ion SiR_3+ through *p*-π conjugate effect. S_N2 nucleophilic attack of **2** at silicon atom of siloxy-alkyne is the initial step of the SMH mechanism. We divide the SMH mechanism into two parts for convenient, the first part (part I) is Ag+ induced SiR_3+ and proton exchange between siloxy-alkyne **1** and amide **2**, which lead to $AgNTf_2$ coordinated ketene **INT3A** and silyl-imine **INT3B**; the second part (part II) is nucleophilic addition between **INT3A** and **INT3B** to form **INT4A**, following with a silylium migration afford final product ***Z*-3** (Scheme 2). By its nature, this is an Ag+ and SiR_3+ exchange process, which have emerged as useful catalytic method, especially for unique transformations hardly accessible to Lewis acid[22-23].

4.3. Formation of ketene and silyl-imines.

Complexation of $AgNTf_2$ with **1a** makes silicon atom of TIPS group susceptible to S_N2 nucleophilic attack by carbamate **2a**. The barrier of this process (**TS1**) is only 18.3 kcal/mol (figure 2). Unlike common S_N2 reaction in organic chemistry, this process leads to five coordinated silicon complex **INT1**, which then dissociate into silver-ketene **INT2a** and TIPS+ coordinated carbamate **INT2b.** The relatively large size and the *d*-orbital of silicon atom contributed the S_N2 process[34-35]. The strong interaction between Ag+ and π-bond make silver-ketene **INT2a** a very good leaving group which also promoted this process[22].

Formation of **INT2a** convert initial siloxy-alkynes **1a** into a strong nucleophile[33], the nucleophile index N_{1a} =3.2, while the nucleophile index N_{int2a} =7.2. Polarity inversion of **1a** take place in this process. The electron transferred from the hydrogen atom of carbamate **2a** into C-Ag bond of the **INT2a.** NBO charge distributions shows that the natural charge of C-Ag changed from 044e to -0.16e from **INTa** to **INT2a**, and the natural charge of hydrogen in the carbamate **2a** changed from 0.16e to 0.46e. In the **INT2b** the hydrogen atom of the nitrogen atom has been activated into proton by TIPS+.

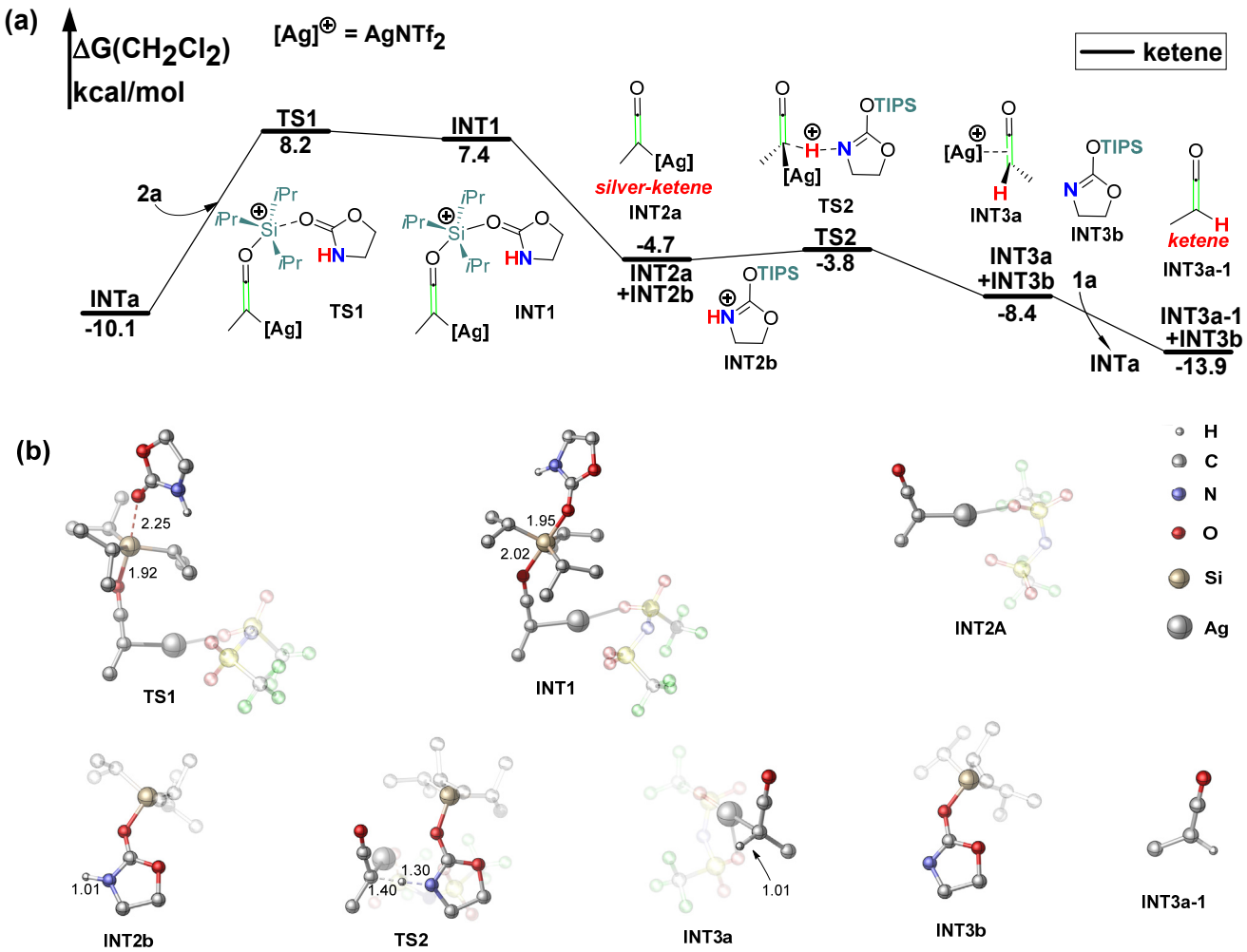

Figure 2. formation ketene **INT3a-1** and silyl-imines **INT3b**. Gibbs energies are in kcal/mol. **a**. Gibbs free energy profile. **b.** Optimized geometries. The hydrogen atom was omitted, and NTf_2- anion was set to transparent for clarity. Except **TS1** and **INT1**, the isopropyl of triisopropylsilyl (TIPS) group was set to transparent for clarity.

Our previous work has shown that Ag+ can activate TIPS group into TIPS+ through *p*-π conjugation. In this reaction Ag+ activate TIPS into TIPS+, TIPS+ then activate the hydrogen atom into proton through *p*-π conjugation, the net effect is Ag+ activate hydrogen atom into proton, which can be regarded as a π-acid and σ-acid exchange scheme.

The proton transfer between the **INT2b** and C-Ag bond of **INT2a** is energetically highly feasible with a barrier (**TS2**) only 0.9 kcal/mol, leading to silyl-imine **INT3b** and $AgNTf_2$ coordinated ketene **INT3a**. The electron transferred from electron-rich C-Ag bond into proton in this process, NBO charge distribution shows that the natural charge of C-Ag changed from -0.16e to 0.11e, and natural charge of hydrogen atom changed from 0.46e to 0.30e. The net effect of this reaction is the $AgNTf_2$ promoted proton and TIPS+ exchange between siloxy-alkyne **1a** and carbamate **2a** to form ketene **INT3a-1** and silyl-imine **INT3b**. Ketene **INT3a-1** and silyl-imine **INT3**b is energetically 2.8kcal/mol more stable than siloxy-alkyne **1a** and carbamate **2a**.

4.4. Silylium ion Migration leads to final product.

Hydroamination or hydroamidation of allenes is quite easy for high activity of the two cumulated π-bond[1, 12, 21]. Ketene is analogs of allenes, it's very important intermediate in the organic chemistry[36-39]. Transition metal promoted nucleophilic attack favors take place in the intersection point of the two π-bond. The barrier (**TS3**) of C-N formation leads to **INT4a** is only 8.8kcal/mol. The nucleophilicity of **INT3b** is higher than **2a** (the nucleophilicity *N*-index of imide N_{int3b} = 2.81, while N_{2a} = 1.86), which contributed to this process. The electron transferred from Si-O to Ag-C in this process. NBO charge distribution shows that the national charge of C-Ag changed from 0.01e to -0.14e, and the natural charge of Si-O changed from 1.22e to 1.32e. The bond length of Si-O changed from 1.72Å to 1.79Å (Figure 3b), which implies the bond between silicon and oxygen is weakened. Actually, the migration of

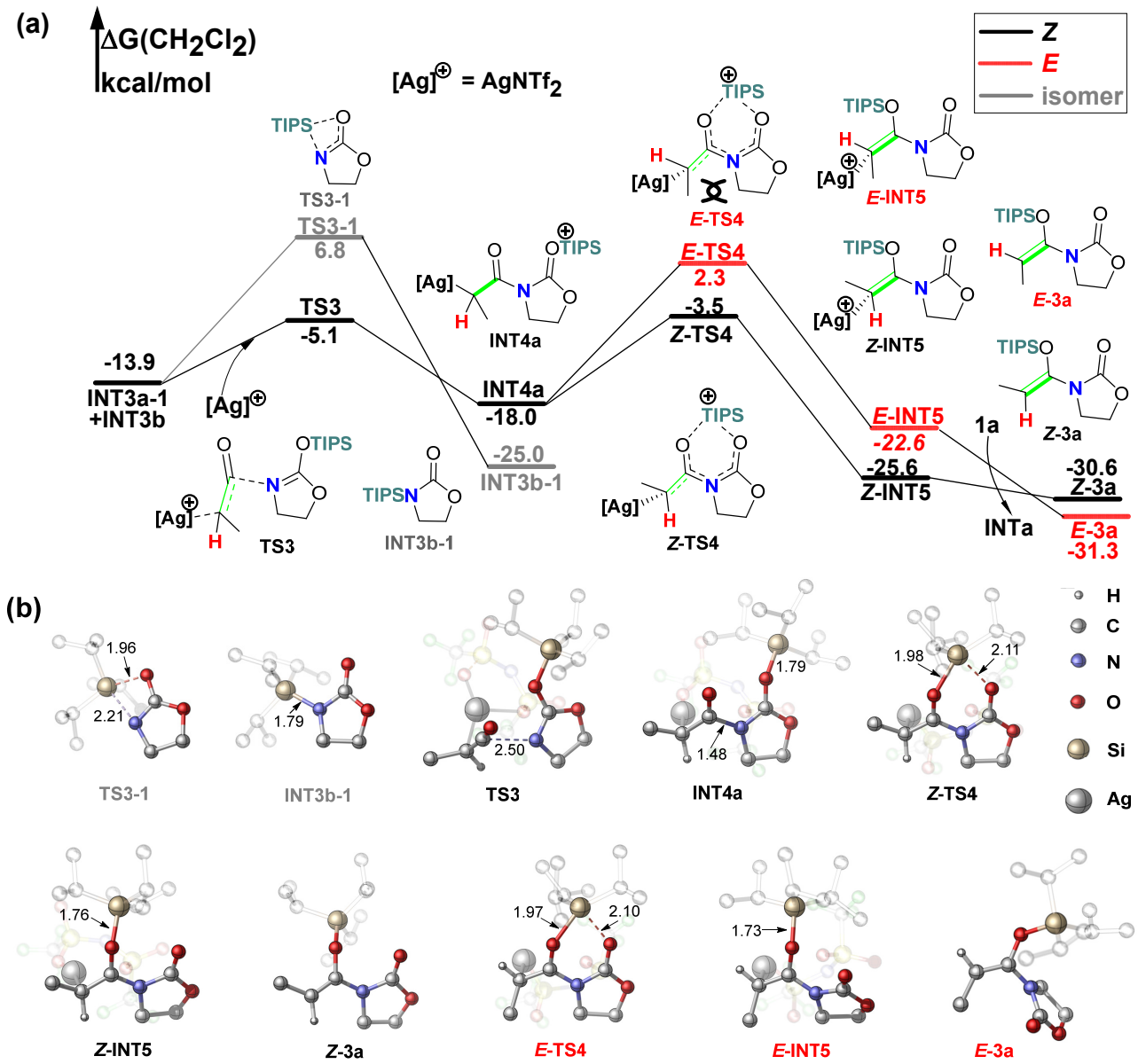

Figure 3. (a) Reaction profiles of formation final product ***Z*-3a**. Gibbs free energies are in kcal/mol. (b) Optimized geometries, the hydrogen atom was omitted, NTf_2- anion and the isopropyl of triisopropylsilyl (TIPS) group was set to transparent for clarity.

TIPS group to obtain $AgNTf_2$ coordinated product ***Z*-INT5** is quite easy with a barrier (***Z*-TS4**) only 14.5kcal/mol. In the ***Z*-TS4** the two carbonyl group are almost in the same plane, and the five *p*-orbitals constitute a large π-delocalized system which lowers the TIPS transfer barrier. After formation of ***Z*-int5**, electron transferred from C-Ag to Si-O. NBO charge distributions show that the natural charge of C-Ag change from -0.14e to 0.04e and Si-O change from 1.32e to 1.26e. The TIPS migration leads to *trans*-hydroamidation product ***E*-3a** is relatively energetically disfavored, the barrier (***E*-TS4**) of this step is 5.8kcal/mol higher than ***Z*-TS4**, which is mainly caused by the relatively larger size of methyl group. The transition states (***Z*-TS4** and ***E*-TS4**) of the TIPS migration step favor planar configuration and form a big delocalized π-system, which increase the repulsion between methyl and methylene. Noncovalent interaction (NCI) analysis[30] was performed to analyze the repulsion between the methyl and methylene groups in the ***E*-TS4,** as indicated in the Figure 4**,** there is a large red area between the two groups, while in the ***Z*-TS4** the red area is much smaller, indicating a more pronounced steric effect in the ***E*-TS4**.

Our calculation is excellent in accordance with experimental observations. Kozmin *et al.* claimed that the ynamides and simple internal alkynes are unreactive in the same conditions. This is a strong support of our proposed SMH mechanism, which highlight the importance of the silylium ion Migration. Ynamides is electron richer than

siloxy-alkyne, if this reaction take place through the author proposed NUA mechanism, the ynamides should be more reactive. Furthermore, using deuterated amide **2a**, no primary deuterium isotope effect (k_H/k_D=1.03) was observed, which means that hydrogen migration is not the rate determine step. Our calculations shows that silylium ion migration (**TS1**) is the rate determine step in this reaction, if we reduce the size of silyl group, the reaction rate may be accelerated.

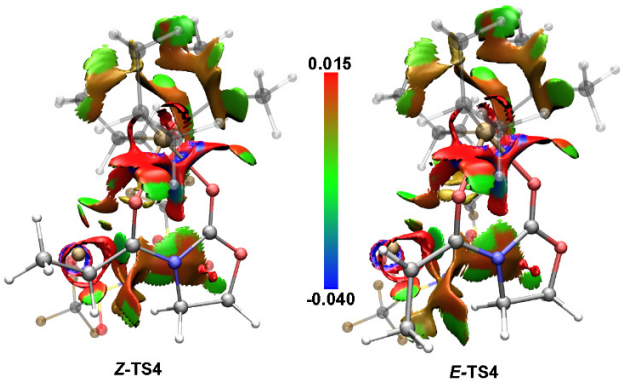

Figure 4. Noncovalent interaction (NCI) analysis of origins of cis-selectivity (red, strong repulsion; green, weak attraction; blue, strong attraction).

4.5. A general way to synthesis substituted enamides.

This reaction goes through relatively independent two steps. In the first step, $AgNTf_2$ convert siloxy-alkyne **1** and amide **2** into ketene **INT3A-1** and silyl-imine **INT3B** (scheme 2). In the second step, $AgNTf_2$ promote nucleophilic addition between ketene **INT3A-1** and silyl-imine **INT3B**, following with a silylium ion migration to afford final product. If the hydrogen atom of ketene was changed into halogen or other groups, this reaction may also take place, and the regio-selective is steric-controlled (scheme 3a). Synthesizing substituted-ketenes has been extensively studied[36-38], and silyl-imines can be easily obtained (One of the feasible approaches is reaction between Chlorotriisopropylsilane (ClTIPS) and amide with base as catalyst in low temperature). So, our calculation provides a general approach to obtain substituted enamides (Scheme 3). Note that the barrier of **INT3b** tautomerize into **INT3b-1** through intramolecular TIPS migration is only 22.8 kcal/mol (figure 3a, with **INT4a** as reference point), once the thermodynamically more stable **INT3b-1** is formed, the barrier of reverse reaction lead to **INT3b** is as high as 31.8kcal/mol, which means that the smallest substituent R7 of ketene **A-INT3A-1** should not be too large to ensure formation of ***Z*-A-3** is kinetically more favored (Scheme 3a). In the ***Z*-TS4** and ***E*-TS4** (figure 3), the movement of methylene of **2a** is constrained by five-membered ring**,** which also increase steric effect, the noncyclic silyl-imine may be better tolerated in this rection.

This method could also be used to obtain the two amino (or acylamino) group substituted alkynes ***Z*-B-3** with ketene imines **B-INT3A-1** and silyl-imine **INT3B** as substrates (scheme 3b). The regio-selectivity get rather complicate. In this case, the steric-effect of R7 and R2, and steric effect of R6 and R4 together determine the ΔG of *cis*-configuration transition state ***Z*-B-TS4**. Similarly, steric effect between R6 and R2, and steric effect between R7 and R4 together determines the ΔG of the *trans*-configuration transition state ***E*-B-TS4**. Our calculations reveal that when *N*-acetyl-substituted ketene imines **B-int3a-1** and TMS-substituted imine **TMS-INT3b** is used as model substrate, the regio-selectivity is reduced compared with previous example (*cis*-selectivity vs *trans*-selectivity = 9.0 kcal/mol vs 11.4 kcal/mol, see details in SI, **figure S1**).

In the reactions we have studied in the Scheme 3, silyl-group of **INT3B** was activated into silylium ion through *p*-π conjugate effect. So, the substrates contain such *p*-π conjugation segment may be also suitable for this reaction (Scheme 3c). We choose silyl-1,2-diazole **C-INT3b** as model to verify this speculate (see details in Figure S2). Our calculations shows that **C-INT3b** can react with ketene **INT3A-1** to afford desired product with a rate determine barrier only 10.6 kcal/mol (see details in SI, Figure S2).

Scheme 3. Methods to obtain substituted enamides.

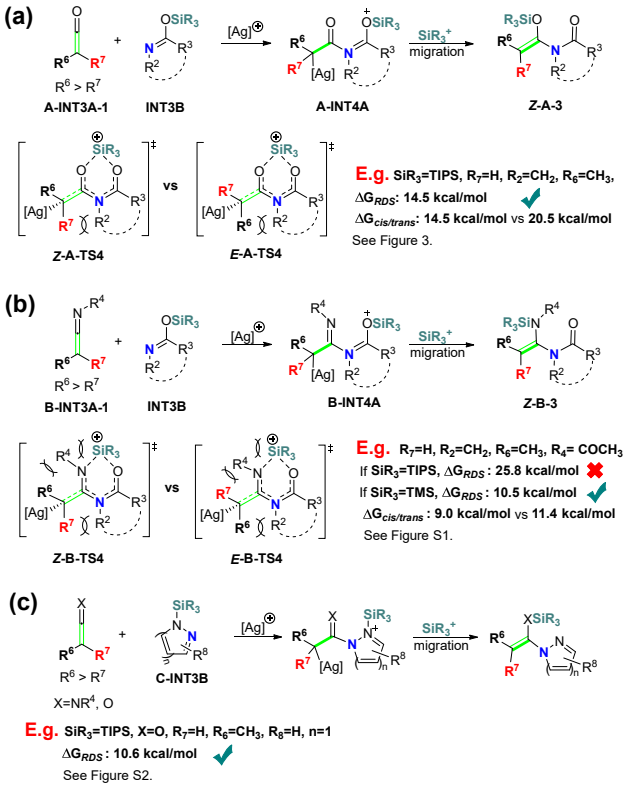

4.6. Substrate scopes of SMH pathway.

According to our proposed SMH mechanism, there are rooms to expand scopes of alkynes. For example, if we change siloxy-alkyne into *N*-silyl protected ynamide (or ynamine) **B-1**, this reaction may also take place (Scheme 4a). We use carbamate **2a** and *N*-TMS substituted ynamide **B-TMS-1** as model to clarify this point of view (see details in SI, Figure S3), our calculations shows that the hydroamidation of **B-TMS-1** through SMH pathway is quite easy with a rate determine barrier (RDB) only 18.0 kcal/mol.

Scheme 4. Possible scopes of alkynes and *p*-*π* conjugation system.

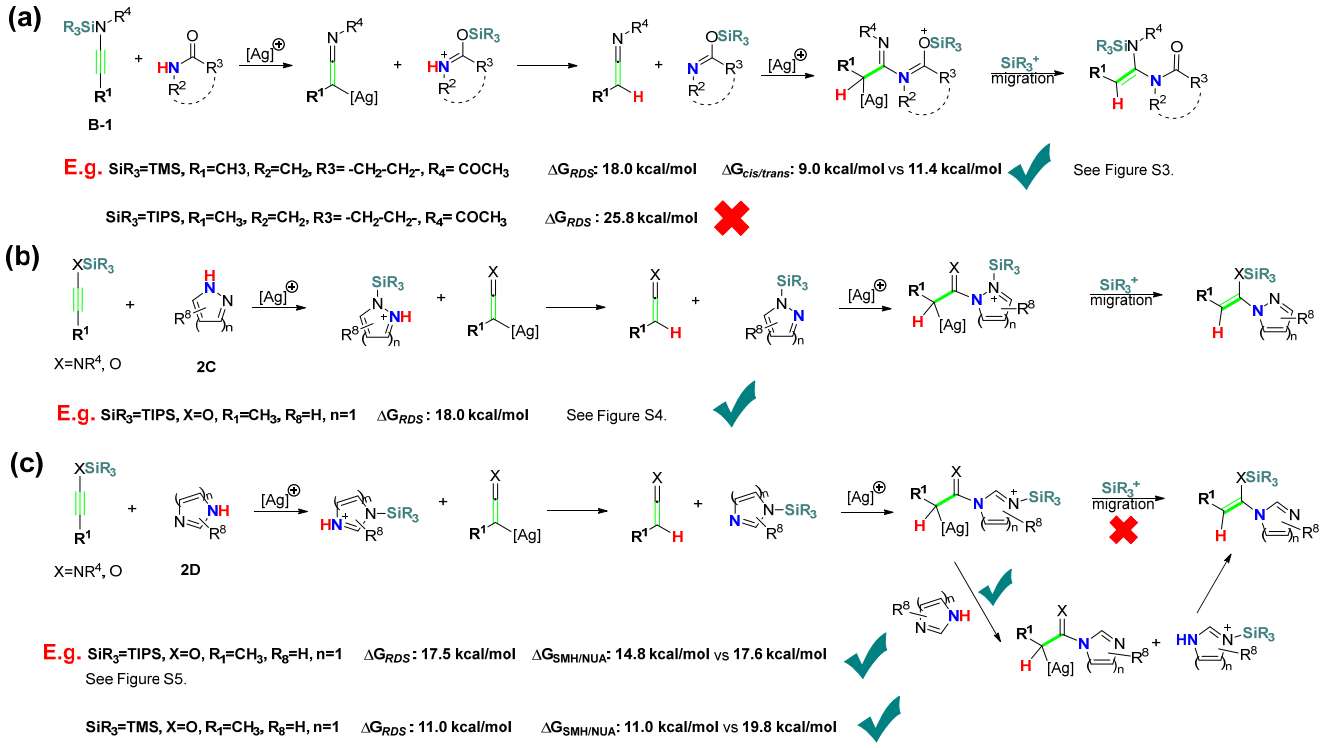

Hydroamidation of **B-1** is very sensitive to the volume of silyl group, when use TIPS substituted ynamide **B-TIPS-1**, this reaction does not take place for the relatively high barrier of silylium ion migration step (25.8 kcal/mol, Scheme 4a), which is mainly caused by steric effect between TIPS and -acetyl. Due to higher barrier of silylium ion migration step, the isomerization of **INT3b** occurs preferentially (22.8 kcal/mol vs 25.8 kcal/mol).

In our proposed SMH pathway, hydrogen atom of amide **2** was activated into silylium ion through *p*-*π* conjugate effect, which implies that some cyclic-*p*-*π* conjugation system, such as diazoles, triazoles, 1H-1,2-diazepine, 1H-1,3-diazepine and so on, may also be suitable substrates for this reaction (see Scheme 4b and Scheme 4c). For example, hydroamination of siloxy-alkyne **1a** with 1,2-diazole is quite easy with a rate-determine barrier 18.0 kcal/mol (see details in SI, Figure S4). As for 1,3-diazoles, the silylium ion migration of last step take place through S_N2 pathway, with a rate determine barrier 18.0 kcal/mol (see details in SI, Figure S5). The NUA process can be eliminated by reduce the volume of SiR_3 group (Scheme 4c).

Conclusion

Catalyzed hydroamidation of internal alkynes meet limited success yet. Our proposed SMH pathway provides a different perspective to catalyze hydroamidation of siloxy-alkynes, *N*-silyl-protected ynamides or *N*-silyl-protected ynamines. Our proposed SMH mechanism can be divided into two steps, the first step is Ag+ promoted proton and silylium ion (**TIPS**$^+$) exchange between siloxy-alkyne and amide, which lead to ketene and silyl-imine, the second step is Ag+ catalyzed nucleophilic addition between ketene and silyl-imine, following with a silylium ion migration lead to final product. The hydroamidation of *N*-silyl-protected ynamines or *N*-silyl-protected ynamides could be completed through a similar pathway. The protocol of synthesis of ketene (or ketene imines) and silyl-imine have been well documented, which means we can use Ag+ to catalyze ketene (or ketene imines) and silyl-imine to obtain a variety of substituted enamides. The substrate scopes of *N*-H source may not only be limited in amides, other *p*-*π* conjugated system such as 1,2-diazoles, 1,3-diazoles and diazepines may also suitable for this reaction. In SMH pathway, the electron extraction competition between Ag+ and silylium ion (TIPS+) induce every elementary step and lead to final product, which is an important supplement to the silylium ion chemistry.

ASSOCIATED CONTENT

Supporting Information.

This material is available free of charge via the Internet at http://pubs.acs.org."

AUTHOR INFORMATION

Corresponding Author

* *fanhj@dicp.ac.cn*

ORCID

HengdingWang: 0000-0003-4198-6032

HongjunFan: 0000-0003-3406-6932

Notes

The authors declare no competing financial interest.

ACKNOWLEDGMENT

Financial support from National Key Research and Development Program of China (No. 2016YFB0600301), National Natural Science Foundation of China (21673224, 21873096), Chinese Academy of Sciences (XDB17010200).

ABBREVIATIONS

SMH, silylium ion migration mediated hydroamidation; NUA: silver induced nucleophilic addition mechanism

Reference

1. Huang, L.; Arndt, M.; Gooßen, K.; Heydt, H.; Gooßen, L. J., Late Transition Metal-Catalyzed Hydroamination and Hydroamidation. *Chem. Rev.* **2015,** *115* (7), 2596-2697.
2. Goossen, L. J.; Blanchot, M.; Salih, K. S. M.; Goosen, K., Ruthenium-Catalyzed Addition of Primary Amides to Alkynes: A Stereoselective Synthesis of Secondary Enamides. *Synthesis-Stuttgart* **2009,** (13), 2283-2288.
3. Goossen, L. J.; Arndt, M.; Blanchot, M.; Rudolphi, F.; Menges, F.; Niedner-Schatteburg, G., A Practical and Effective Ruthenium Trichloride-Based Protocol for the Regio- and Stereoselective Catalytic Hydroamidation of Terminal Alkynes. *Adv. Synth. Catal.* **2008,** *350* (17), 2701-2707.
4. Goossen, L. J.; Rauhaus, J. E.; Deng, G. J., Ru-catalyzed anti-markovnikov addition of amides to alkynes: A regio- and stereoselective synthesis of enamides. *Angewandte Chemie-International Edition* **2005,** *44* (26), 4042-4045.
5. Rodriguez, A. L.; Koradin, C.; Dohle, W.; Knochel, P., Versatile indole synthesis by a 5-endo-dig cyclization mediated by potassium or cesium bases. *Angewandte Chemie-International Edition* **2000,** *39* (14), 2488-+.
6. Rieder, C. L.; Cole, R., Chromatid cohesion during mitosis: lessons from meiosis. *J. Cell Sci.* **1999,** *112* (16), 2607-2613.
7. Tashrifi, Z.; Mohammadi Khanaposhtani, M.; Biglar, M.; Larijani, B.; Mahdavi, M., Recent Advances in Alkyne Hydroamination as a Powerful Tool for the Construction of C-N Bonds. *Asian Journal of Organic Chemistry* **2020,** *9* (7), 969-991.
8. Neto, J. S. S.; Zeni, G., Alkynes and Nitrogen Compounds: Useful Substrates for the Synthesis of Pyrazoles. *Chemistry-a European Journal* **2020,** *26* (37), 8175-8189.
9. Hannedouche, J.; Schulz, E., Hydroamination and Hydroaminoalkylation of Alkenes by Group 3-5 Elements: Recent Developments and Comparison with Late Transition Metals. *Organometallics* **2018,** *37* (23), 4313-4326.
10. Sengupta, M.; Das, S.; Islam, S. M.; Bordoloi, A., Heterogeneously Catalysed Hydroamination. *Chemcatchem* **2021,** *13* (4), 1089-1104.
11. Reznichenko, A. L.; Nawara-Hultzsch, A. J.; Hultzsch, K. C., Asymmetric Hydroamination. In *Stereoselective Formation of Amines*, Li, W.; Zhang, X., Eds. 2014; Vol. 343, pp 191-260.
12. Fukumoto, Y., Catalytic Hydroamination of C-C Multiple Bonds. *Journal of Synthetic Organic Chemistry Japan* **2009,** *67* (7), 735-750.
13. Serrano-Becerra, J. M.; Maier, A. F. G.; Gonzalez-Gallardo, S.; Moos, E.; Kaub, C.; Gaffga, M.; Niedner-Schatteburg, G.; Roesky, P. W.; Breher, F.; Paradies, J., Mono- vs. Dinuclear Gold-Catalyzed Intermolecular Hydroamidation. *Eur. J. Org. Chem.* **2014,** *2014* (21), 4515-4522.
14. Wong, V. H. L.; Hor, T. S. A.; Hii, K. K., Silver-catalysed intramolecular hydroamination of alkynes with trichloroacetimidates. *Chem. Commun.* **2013,** *49* (81), 9272-9274.
15. Zhang, X.; Zhou, Y.; Wang, H.; Guo, D.; Ye, D.; Xu, Y.; Jiang, H.; Liu, H., Silver-catalyzed intramolecular hydroamination of alkynes in aqueous media: efficient and regioselective synthesis for fused benzimidazoles. *Green Chemistry* **2011,** *13* (2), 397-405.
16. Monge, D.; Jensen, K. L.; Franke, P. T.; Lykke, L.; Jorgensen, K. A., Asymmetric One-Pot Sequential Organo- and Gold Catalysis for the Enantioselective Synthesis of Dihydropyrrole Derivatives. *Chemistry-a European Journal* **2010,** *16* (31), 9478-9484.
17. Kociecka, P.; Czelusniak, I.; Szymanska-Buzar, T., Efficient and Selective Synthesis of E-Vinylamines via Tungsten(0)-Catalyzed Hydroamination of Terminal Alkynes. *Adv. Synth. Catal.* **2014,** *356* (16), 3319-3324.
18. Sun, J.; Kozmin, S. A., Silver-catalyzed hydroamination of siloxy alkynes. *Angewandte Chemie-International Edition* **2006,** *45* (30), 4991-4993.
19. Kuai, C.; Wang, L.; Cui, H.; Shen, J.; Feng, Y.; Cui, X., Efficient and Selective Synthesis of (E)-Enamides via Ru(II)-Catalyzed Hydromidation of Internal Alkynes. *Acs Catalysis* **2016,** *6* (1), 186-190.
20. Lyu, X.; Zhang, J.; Kim, D.; Seo, S.; Chang, S., Merging NiH Catalysis and Inner-Sphere Metal-Nitrenoid Transfer for Hydroamidation of Alkynes. *Journal of the American Chemical Society* **2021,** *143* (15), 5867-5877.
21. Fang, G.; Bi, X., Silver-catalysed reactions of alkynes: recent advances. *Chem. Soc. Rev.* **2015,** *44* (22), 8124-8173.
22. Wang, H.-D.; Fan, H.-J., Silylium ion mediated 2+2 cycloaddition leads to 4+2 Diels-Alder reaction products. *Comm Chem* **2020,** *3* (1), 126-135.
23. Turkmen, Y. E.; Montavon, T. J.; Kozmin, S. A.; Rawal, V. H., Silver-catalyzed formal inverse electron-demand Diels-Alder reaction of 1,2-diazines and siloxy alkynes. *J. Am. Chem. Soc.* **2012,** *134* (22), 9062-9065.
24. Haines, B. E.; Sarpong, R.; Musaev, D. G., Generality and Strength of Transition Metal beta-Effects. *J. Am. Chem. Soc.* **2018,** *140* (33), 10612-10618.
25. Frisch, M. J.; Trucks, G. W.; Schlegel, H. B.; Scuseria, G. E.; Robb, M. A.; Cheeseman, J. R.; Scalmani, G.; Barone, V.; Petersson, G. A.; Nakatsuji, H.; Li, X.; Caricato, M.; Marenich, A. V.; Bloino, J.; Janesko, B. G.; Gomperts, R.; Mennucci, B.; Hratchian, H. P.; Ortiz, J. V.; Izmaylov, A. F.; Sonnenberg, J. L.; Williams; Ding, F.; Lipparini, F.; Egidi, F.; Goings, J.; Peng, B.; Petrone, A.; Henderson, T.; Ranasinghe, D.; Zakrzewski, V. G.; Gao, J.; Rega, N.; Zheng, G.; Liang, W.; Hada, M.; Ehara, M.; Toyota, K.; Fukuda, R.; Hasegawa, J.; Ishida, M.; Nakajima, T.; Honda, Y.; Kitao, O.; Nakai, H.; Vreven, T.; Throssell, K.; Montgomery Jr., J. A.; Peralta, J. E.; Ogliaro, F.; Bearpark, M. J.; Heyd, J. J.; Brothers, E. N.; Kudin, K. N.; Staroverov, V. N.; Keith, T. A.; Kobayashi, R.; Normand, J.; Raghavachari, K.; Rendell, A. P.; Burant, J. C.; Iyengar, S. S.; Tomasi, J.; Cossi, M.; Millam, J. M.; Klene, M.; Adamo, C.; Cammi, R.; Ochterski, J. W.; Martin, R. L.; Morokuma, K.; Farkas, O.; Foresman, J. B.; Fox, D. J. *Gaussian 16 Rev. C.01*, Revision C.01; Gaussian, Inc.: Wallingford, CT, 2016.
26. Chai, J.-D.; Head-Gordon, M., Long-range corrected hybrid density functionals with damped atom-atom dispersion corrections. *Phys. Chem. Chem. Phys.* **2008,** *10* (44), 6615-6620.
27. Weigend, F.; Ahlrichs, R., Balanced basis sets of split valence, triple zeta valence and quadruple zeta valence quality for H to Rn: Design and assessment of accuracy. *Phys. Chem. Chem. Phys.* **2005,** *7* (18), 3297-3305.
28. Fukui, K., The path of chemical reactions - the IRC approach. *Acc. Chem. Res.* **1981,** *14* (12), 363-368.
29. Legault, C. Y. *CYLview, 1.0b*, Université de Sherbrooke: 2009.
30. Johnson, E. R.; Keinan, S.; Mori-Sánchez, P.; Contreras-García, J.; Cohen, A. J.; Yang, W., Revealing Noncovalent Interactions. *Journal of the American Chemical Society* **2010,** *132* (18), 6498-6506.
31. Lu, T.; Chen, F., Multiwfn: A multifunctional wavefunction analyzer. *J. Comput. Chem.* **2012,** *33* (5), 580-592.
32. Humphrey, W.; Dalke, A.; Schulten, K., VMD: Visual molecular dynamics. *Journal of Molecular Graphics & Modelling* **1996,** *14* (1), 33-38.
33. Domingo, L. R.; Rios-Gutierrez, M.; Perez, P., Applications of the

Conceptual Density Functional Theory Indices to Organic Chemistry Reactivity. *Molecules* **2016,** *21* (6), 748-769.
34. Lee, V. Y., Tricoordinate silyl cations (silylium ions). *Russ. Chem. Rev.* **2019,** *88* (4), 351-369.
35. Mueller, T., Silylium Ions. In *Functional Molecular Silicon Compounds I: Regular Oxidation States*, Scheschkewitz, D., Ed. Springer: New York, 2014; Vol. 155, pp 107-162.
36. Huang, L.; Wu, J.; Hu, J.; Bi, Y.; Huang, D., Ketene dithioacetals in organic synthesis. *Tetrahedron Lett.* **2020,** *61* (4), 151363-1513776.
37. Allen, A. D.; Tidwell, T. T., Recent advances in ketene chemistry. *Arkivoc* **2016,** *i*, 415-490.
38. Allen, A. D.; Tidwell, T. T., Structure and Mechanism in Ketene Chemistry. In *Adv. Phys. Org. Chem.*, Ian H. Williams, N. H. W., Ed. 2014; Vol. 48, pp 229-324.
39. Minnihan, E. C.; Colletti, S. L.; Toste, F. D.; Shen, H. C., Gold(I)-Catalyzed regioselective cyclizations of silyl ketene amides and carbamates with alkynes. *J. Org. Chem.* **2007,** *72* (16), 6287-6289.